Relative Tropospheric Photolysis Rates of Acetaldehyde and Formaldehyde Isotopologues Measured at the European Photoreactor Facility

Elna J. K. Nilsson,[†] Lihn Bache-Andreassen,[‡] Matthew S. Johnson,[†] and Claus J. Nielsen*[,‡]

Copenhagen Center for Atmospheric Research, Department of Chemistry, University of Copenhagen, Universitetsparken 5 DK-2100 Copenhagen OE, Denmark, and Centre for Theoretical and Computational Chemistry, Department of Chemistry, University of Oslo, Pb. 1033 - Blindern 0315 Oslo, Norway

Received: December 16, 2008; Revised Manuscript Received: February 16, 2009

The photolysis rates of HCHO, DCDO, CH_3CHO, and CH_3CDO are studied by long-path FTIR spectroscopy in natural tropospheric conditions at the European Photoreactor Facility (EUPHORE) in Valencia, Spain. Average relative photolysis rates $j_{HCHO}/j_{DCDO} = 3.15 \pm 0.08$ and $j_{CH_3CHO}/j_{CH_3CDO} = 1.26 \pm 0.03$ are obtained from three days of experiments for each reaction in the period June 17 to July 7, 2006.

1. Introduction

Acetaldehyde and formaldehyde are key atmospheric trace gases that are formed in the photochemical oxidation of hydrocarbons of both natural and anthropogenic origins.[1] The aldehydes are also emitted in fossil fuel combustion and biomass burning.[2]

Substantial amounts of acetaldehyde (100 ppt) are found up to altitudes of 12 km. Acetaldehyde photochemistry is an important source of HO_x in the free troposphere.[3,4] Photolysis of acetaldehyde has three product channels: [5,6]

$$CH_3CHO + h\nu \rightarrow CH_3 + HCO \qquad (\lambda \leq 330\ \text{nm}) \tag{1a}$$

$$CH_3CHO + h\nu \rightarrow CH_4 + CO \qquad (\lambda \leq 292\ \text{nm}) \tag{1b}$$

$$CH_3CHO + h\nu \rightarrow CH_3CO + H \qquad (\lambda < 320\ \text{nm}) \tag{1c}$$

At tropospheric conditions only the first product channel (1a) is of importance. Channel 1c has very small quantum yields (0.025 at 300 nm, decreasing to zero at 320 nm) and does not contribute significantly.[5,6]

Formaldehyde plays a key role in atmospheric photochemistry: its photolysis proceeds via two pathways at atmospherically relevant wavelengths and constitutes an important source of HO_x and molecular hydrogen:[7−10]

$$HCHO + h\nu \rightarrow H + HCO \qquad (\lambda \leq 330\ \text{nm}) \tag{2a}$$

$$HCHO + h\nu \rightarrow H_2 + CO \qquad (\lambda \leq 361\ \text{nm}) \tag{2b}$$

The quantum yields of both reactions depend on wavelength and (2b) also depends on pressure, and thus the photolysis rates j_{2a} and j_{2b} vary throughout the atmosphere. Under average tropospheric conditions, however, the two photolysis pathways are of roughly equal importance.[5,6,11]

Measurements of the isotopic composition of atmospheric trace gases are used to infer the photochemical history of sampled air masses, leading to a better understanding of the sources and sinks of these compounds.[12,13] Isotopic analysis is used to refine the global budgets of greenhouse gases.[14,15] Isotope effects are useful and sensitive benchmarks for quantum chemical calculations because they provide additional information about the bottlenecks of reactions. Formaldehyde has been the subject of intense recent interest regarding the mechanism of its dissociation,[16−19] including the "wandering H-atom" mechanism.[20]

We have previously shown that the formaldehyde and acetaldehyde reactions with OH, Br, Cl, and NO_3 radicals exhibit large hydrogen/deuterium kinetic isotope effects (KIEs).[21−25] Likewise the UV spectra of formaldehyde[26,27] and acetaldehyde[28] are modified by isotopic substitution. Significant isotope effects in the tropospheric photolysis rates of formaldehyde have been demonstrated:[29,30] tropospheric HCHO photolysis is about 3 times faster than that of DCDO[29] and 1.5 times faster than that of HCDO.[30,31] Significant fractionation in atmospheric photolysis of formaldehyde depletes D in the molecular hydrogen product,[30] and this effect decreases with altitude.[32] However, the $\delta D(H_2)$ of atmospheric molecular hydrogen is larger than $\delta D(CH_4)$ of atmospheric methane.[33] This is explained by isotope effects in the reaction steps from CH_4 to HCHO, enriching deuterium in the final product relative to its abundance in methane.[34]

The UV absorption cross sections of HCHO have been studied numerous times and have been critically reviewed.[5,6] Recently, quantitative high resolution UV data have been published,[35−37] and we have presented absolute absorption cross sections in the UV (300−360 nm) and infrared (3200−1500 cm^{-1}) regions of HCHO, HCDO, and DCDO using simultaneous measurements in both spectral regions.[27] A key result in relation to the very different tropospheric photolysis rates of the formaldehyde isotopomers is that their integrated UV cross sections are equal to within the experimental uncertainty.

The UV absorption cross sections of CH_3CHO have also been studied numerous times and have been critically reviewed.[5,6] The $n \rightarrow \pi^*$ band in acetaldehyde is broad with some vibrational structure and a maximum around 290 nm. The band is a superposition of S_0-S_1 (240−290 nm) and the spin forbidden

* Corresponding author. Fax: +47 2285 5441. E-mail address: claus.nielsen@kjemi.uio.no.
[†] University of Copenhagen.
[‡] University of Oslo.

10.1021/jp811113c CCC: $40.75
Published on Web 03/19/2009

S_0-T_1 (255−337 nm) transitions.[38] The single report on the n → π* band in the acetaldehyde isotopologues CH_3CDO and CD_3CDO shows large isotope effects in the region below 300 nm; the heavy isotopologues have smaller cross sections at all wavelengths.[28]

In the present work we report the first results for isotope effects in the tropospheric photolysis of acetaldehyde. We have also reinvestigated the photolysis rate of DCDO relative to HCHO. The motivation for reinvestigating the formaldehyde photolysis is to test the validity of our earlier work under different conditions and to investigate the role of the wall source of HCHO,[39] which was not considered in the earlier study.[29] The difference in conditions includes changes in temperature, actinic flux, and solar zenith angle because the present study was conducted under cloudy conditions about a month earlier in the year (June 2006) than the previous study (July 2004). Also, during the earlier work the EUPHORE A chamber was used whereas for the present work the EUPHORE B chamber was used. The two chambers differ in that the A chamber operates at constant pressure and the B chamber work at constant inflow of purified air.

2. Experimental Section

The photolysis experiments were carried out in the period June 17 to July 7, 2006, in chamber B at the European Photoreactor Facility (EUPHORE) in Valencia, Spain (longitude −0.5, latitude +39.5). The present experiments are similar to those described in our recent reports of the photolysis of formaldehyde isotopologues.[29,30] A typical experiment starts around 06:00 UT (local time = UT + 2) when reagents are added to the chamber. The canopy of the chamber is opened after 1−2 h when a series of spectra of the dark chamber have been recorded and the reagents are considered to be well-mixed. Depending on the photolysis rates of the reagents, the experiment lasts up to 4 h after which the chamber is closed and flushed overnight with scrubbed air.

For the formaldehyde experiments approximately 250 mg of HCHO and 250 mg of DCDO (corresponding to a volume fraction of about 800 ppb each in the chamber) were added simultaneously by heating the mixed paraformaldehyde polymers to 160 °C and flushing the vapors into the chamber. For the acetaldehyde experiments between 0.3 and 0.5 mL (650 ppb to 1.1 ppm) of each of CH_3CHO and CH_3CDO were evaporated and flushed into the chamber. Throughout the duration of the experiment the actinic flux (290−520 nm) was measured by a Bentham DM300 spectroradiometer, and IR spectra were recorded every 15 min by coadding 230 interferograms obtained at a resolution of 0.5 cm^{-1} (Nicolet Magna 550 FTIR spectrometer coupled with a White-type multireflection mirror system with an optical path length of 553.3 m). In each experiment, the analysis of the gas mixture was started at least 30 min before exposing the mixture to sunlight to check for dark reactions.

Purified air is constantly added to compensate for leakage, loss through connections and continuous sampling by ozone and NO_x monitors. This is corrected for in the data analysis: SF_6 is added to measure the dilution rate. The apparent dilution rate coefficient of the chamber, $k_{dilution}$, was determined in each experiment by adding ca. 20 ppb SF_6 gas to the chamber and monitoring its concentration by FTIR:

$$\ln\{[SF_6]_0/[SF_6]_t\} = k_{dilution} \cdot t \quad (3)$$

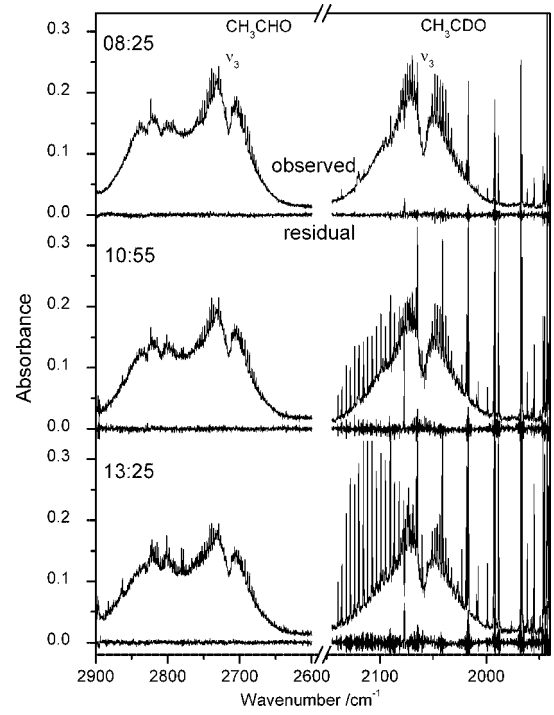

Figure 1. Observed spectra of the CH and CD stretching regions in CH_3CHO and CH_3CDO (overlapped by the sharp lines of the CO band centered at 2143 cm^{-1} and a few H_2O lines), and residuals of fit during the photolysis experiment in the EUPHORE chamber B on June 21, 2006. See text for information on the spectral fitting procedure.

where $[SF_6]_0$ and $[SF_6]_t$ are the SF_6 concentrations at times zero and t, respectively. Typical values of $k_{dilution}$ of the EUPHORE Chamber B during the present experiments are in the range of $(6-7) \times 10^{-6}$ s^{-1}. Variations in pressure, temperature, solar flux, j_{NO_2}, [NO], $[NO_2]$, $[O_3]$, and [CO] in the chamber during an experiment are documented for June 19, 2006, in Figures S1−S8 (Supporting Information).

The formaldehyde isotopologues used were in the form of paraformaldehyde, $(CH_2O)_n$. The samples were commercial products: HCHO (Fluka, extra pure) and DCDO (CDN, 99.8 atom % D). The liquid acetaldehyde samples were commercial products: CH_3CHO (Fluka, >99.0% purity) and CH_3CDO (CDN, 99.9% purity, 99.6 atom % D).

3. Results

The experimental spectra were analyzed using a nonlinear least-squares spectral fitting program, MALT.[40] In this method, the spectrum of the mixture of absorbing species is first simulated by calculation from initial estimates of the absorber concentrations. The calculation is then iterated to minimize the residual between the measured and simulated spectra. In the spectrum calculation, absorption coefficients are normally calculated from HITRAN line parameter data,[41] the transmission spectrum is computed and then convolved with the FTIR instrument function to simulate the measured spectrum. If HITRAN line parameter data are not available, a laboratory spectrum measured at high resolution may be used. The iterative fitting follows the Levenberg−Marquardt algorithm to adjust the calculation parameters (absorber concentrations, continuum level and instrument line-shape parameters) and achieve a least-squares minimum residual between measured and simulated spectra in typically 5−10 iterations.

The spectral features used in the analysis of the formaldehyde removal from the chamber were the C−H stretching bands of

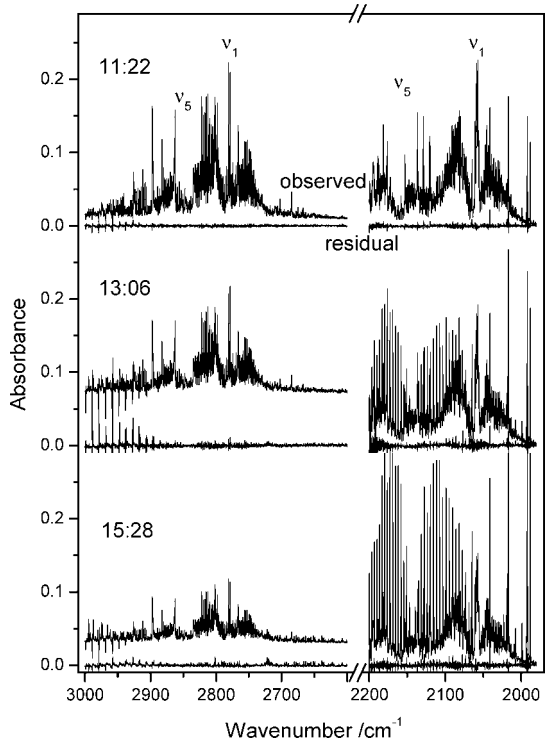

Figure 2. Observed spectra of the ν_1 and ν_5 bands af HCHO and DCDO (overlapped by the sharp lines of the CO band centered at 2143 cm^{-1} and a few H_2O lines), and residuals of fit during the photolysis experiment in the EUPHORE chamber B on June 19, 2006. See text for information on the spectral fitting procedure.

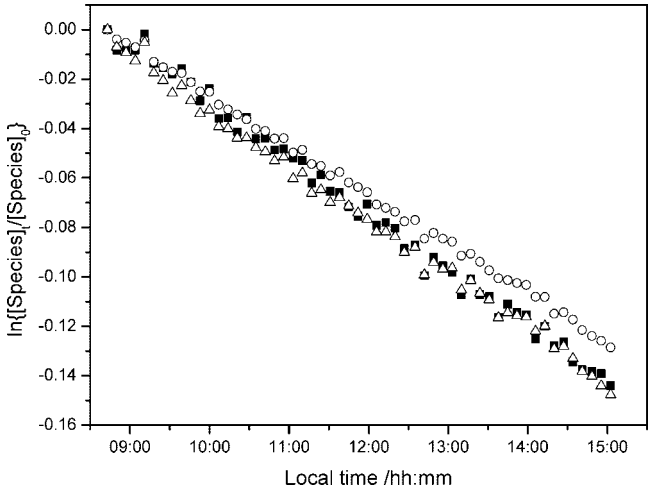

Figure 3. Decay curves for SF_6 (■), HCHO (○), and DCDO (Δ) in the EUPHORE reactor B on June 27, 2006. Initial volume fractions of HCHO and DCDO are 890 and 730 ppb, respectively.

HCHO in the 3000−2600 cm^{-1} region and the C−D stretching bands of DCDO in the 2200−1980 cm^{-1} region. Experimental high-resolution IR spectra of HCHO and DCDO[21] were used in the analyses. The spectral features used in the analysis of the acetaldehyde removal from the chamber were the C−H stretching bands in the 2900−2600 cm^{-1} region and the C−D stretching bands in the 2145−1940 cm^{-1} region. High-resolution IR spectra of HCHO,[21] and CH_3CHO and CH_3CDO obtained in the present work were used in the fitting procedure. For H_2O and CO the spectral data needed in the fitting procedure were taken from the HITRAN 2004 database.[41] Figures 1 and 2 show an example of the spectral fitting at the beginning, the middle and the end of acetaldehyde and formaldehyde photolysis experiments.

The concentration of SF_6 was determined from the integrated intensity of its $\nu_3(F_{1u})$ band around 947.5 cm^{-1}, the shape of which is sensitive to temperature variations. We have previously shown that spectral overlap with HCHO and DCDO is negligible in the region of integration.[29] Also for the acetaldehydes in question the spectral overlap is negligible.

To check for possible interfering heterogeneous processes in the chamber, the loss of formaldehyde was measured relative to that of SF_6 with the chamber canopy closed. Figure 3 shows normalized decay curves of SF_6, HCHO and DCDO as a function of time. The decay rate for HCHO is slightly less than the (virtually identical) decay rates of DCDO and SF_6. This indicates a "dark" source, W_{HCHO}, of HCHO in the chamber, and assuming the source to be constant with time the decay of HCHO is described by

$$\frac{d[HCHO]}{dt} = -k_{dilution}[HCHO] + W_{HCHO} \quad (4)$$

which may be solved to give

$$[HCHO]_t = [HCHO]_0 \cdot \exp^{-k_{dilution} \cdot t} + \frac{W_{HCHO}}{k_{dilution}} \cdot (1 - \exp^{-k_{dilution} \cdot t}) \quad (5)$$

The dark source may be quantified from the data in Figure 3 (once the HCHO starting concentration and the dilution rate, $k_{dilution}$, are known) to be approximately 0.5 ppt s^{-1}. This is comparable to the additional HCHO source reported for the chamber opened to sunlight;[39] see below.

With the chamber canopy open, OH radicals are formed as hydrogen atoms and formyl radicals from the aldehyde photolysis react with O_2 to generate HO_2 and eventually H_2O_2, OH, and O_3. As there is always a small amount of NO_x present, depending in part on outside conditions, these reactions could potentially generate enough OH that the OH + HCHO and OH + CH_3CHO reactions would compete with photolysis; see Figures S5−S7 (Supporting Information). It is obviously important to quantify the fraction of the aldehydes that reacts with OH because not only is it a loss process but it is also associated with a kinetic isotope effect, $k_{OH+HCHO}/k_{OH+DCDO} = 1.66$[21] and $k_{OH+CH_3CHO}/k_{OH+CH_3CDO} = 1.42$,[22] which will influence the result. The reaction system was therefore examined using a FACSIMILE kinetic model based on the Master Chemical Mechanism and specially designed for the EUPHORE chamber to examine the extent of the competing chemical reaction of the aldehydes with OH.[42] The model uses the temperature and the photolysis rate of NO_2 recorded in the chamber each day, and the initial concentrations of NO_x, O_3, and (in the present case) HCHO or CH_3CHO to simulate the OH concentration throughout the day for each day of experiments. The j_{NO_2} values, Figure S4 (Supporting Information), are used to scale the photolysis rates of all species in the model to match the specific conditions of a given day. As mentioned, the formaldehyde experiments in this study were carried out under cloudy conditions and the j_{NO_2} values are around 50% lower than in the previous study of the HCHO/DCDO photolysis.[29] Figure 4 shows calculated OH radical concentrations as a function of time. The calculated OH concentrations in the reaction chamber during experiments are not extremely high and contribute only slightly to the loss of the aldehydes. However, as much as 10^6 cm^{-3} may be generated in the middle of the day in some

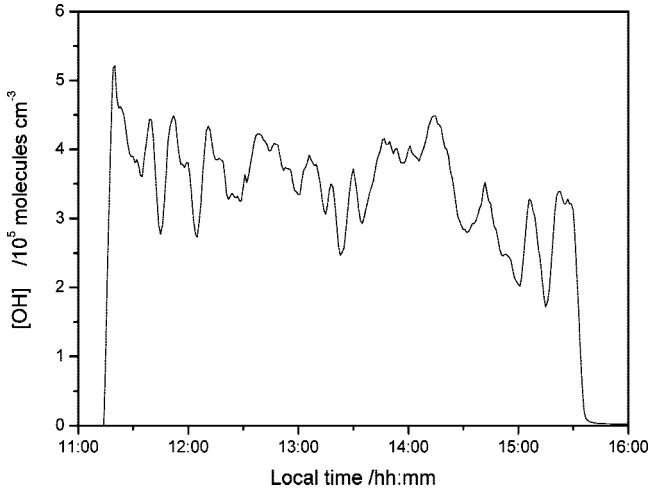

Figure 4. Calculated concentration of OH radicals inside the EUPHORE chamber B on June 19, 2006. The chamber canopy was opened at 11:22 and closed at 15:36 (local time = UT+2). See text for description of the model.

experiments and the modeled OH concentration is used to make the appropriate corrections in the data analyses; see below.

The relative rate method was used to determine the photolysis rates of DCDO and CH_3CDO relative to those of HCHO and CH_3CHO. The decays of the concentrations of the species undergoing photolysis are measured simultaneously as a function of reaction time. Consider an ideal situation with two simultaneous photolysis processes with the rates j_{RH} and j_{RD}, where RH denotes the normal species and RD the deuterated species:

$$\begin{aligned} \mathrm{RH} + h\nu &\xrightarrow{j_{RH}} \text{products} \\ \mathrm{RD} + h\nu &\xrightarrow{j_{RD}} \text{products} \end{aligned} \tag{6}$$

Assuming that there are no loss processes other than these reactions and that there are no other processes producing the reactants, the following relation is valid:

$$\ln\left\{\frac{[\mathrm{RH}]_0}{[\mathrm{RH}]_t}\right\} = \frac{j_{RH}}{j_{RD}} \ln\left\{\frac{[\mathrm{RD}]_0}{[\mathrm{RD}]_t}\right\} \tag{7}$$

where $[RH]_0$, $[RH]_t$, $[RD]_0$, and $[RD]_t$ denote the concentrations of the aldehydes at times zero and t, respectively. A plot of $\ln([RH]_0/[RH]_t)$ vs $\ln([RD]_0/[RD]_t)$ will thus give the relative photolysis rate coefficient j_{RH}/j_{RD} as the slope.

In the present cases, however, three loss processes for the aldehyde isotopologues in the chamber have to be taken into account (photolysis, reaction with OH, and dilution):

$$\begin{aligned} \frac{\mathrm{d}[\mathrm{RH}]}{\mathrm{d}t} &= -(j_{RH} + k_{\text{dilution}} + k_{\mathrm{OH+RH}}\cdot[\mathrm{OH}])\cdot[\mathrm{RH}] \\ \frac{\mathrm{d}[\mathrm{RD}]}{\mathrm{d}t} &= -(j_{RD} + k_{\text{dilution}} + k_{\mathrm{OH+RD}}\cdot[\mathrm{OH}])\cdot[\mathrm{RD}] \end{aligned} \tag{8}$$

which may be solved to give

$$\ln\frac{[\mathrm{RH}]_0}{[\mathrm{RH}]_t} - k_{\text{dilution}}\cdot t - \int_0^t k_{\mathrm{OH+RH}}\cdot[\mathrm{OH}]_t\cdot\mathrm{d}t = \frac{j_{RH}}{j_{RD}}\left(\ln\frac{[\mathrm{RD}]_0}{[\mathrm{RD}]_t} - k_{\text{dilution}}\cdot t - \int_0^t k_{\mathrm{OH+RD}}\cdot[\mathrm{OH}]_t\cdot\mathrm{d}t\right) \tag{9}$$

In the formaldehyde experiments there is the mentioned HCHO production in the EUPHORE chamber, W_{HCHO}, which has been parametrized in terms of j_{NO_2} and temperature: $W_{HCHO} = (3.1 \times 10^{17}\ \mathrm{cm^{-3}}) \times j_{NO_2} \times \exp(5686/T)$.[39] Although HCHO production in the chamber is small, ~2 ppb h^{-1}, it is not negligible at low HCHO volume fractions. The concentrations of HCHO and DCDO can then be described by

$$\begin{aligned} \frac{\mathrm{d}[\mathrm{HCHO}]}{\mathrm{d}t} &= -(j_{HCHO} + k_{\text{dilution}} + k_{\mathrm{OH+HCHO}}\cdot[\mathrm{OH}])\cdot[\mathrm{HCHO}] + W_{HCHO} \\ \frac{\mathrm{d}[\mathrm{DCDO}]}{\mathrm{d}t} &= -(j_{DCDO} + k_{\text{dilution}} + k_{\mathrm{OH+DCDO}}\cdot[\mathrm{OH}])\cdot[\mathrm{DCDO}] \end{aligned} \tag{10}$$

where k_{dilution} is the dilution rate (see above) and $k_{OH+HCHO}$ and $k_{OH+DCDO}$ are the rate coefficients for the OH reactions with HCHO and DCDO, respectively. Although the actinic flux varies during the experiments, the variation is not large, Figure S3 (Supporting Information). In addition, the variations do not change the shape of the intensity spectrum of the 300−400 nm region, the photoactive range for the two acetaldehyde and the two formaldehyde isotopologues. To a good approximation j_{HCHO} and j_{DCDO} will therefore have the same implicit time dependency, and the above equations may be solved to give the following relation:

$$\ln\frac{[\mathrm{HCHO}]_0}{[\mathrm{HCHO}]_t} - k_{\text{dilution}}\cdot t - \int_0^t k_{\mathrm{OH+HCHO}}\cdot[\mathrm{OH}]_t\cdot\mathrm{d}t + \frac{\langle W\rangle}{[\mathrm{HCHO}]_0}\cdot\frac{\exp(\langle L\rangle\cdot t) - 1}{\langle L\rangle} = \frac{j_{HCHO}}{j_{DCDO}}\left(\ln\frac{[\mathrm{DCDO}]_0}{[\mathrm{DCDO}]_t} - k_{\text{dilution}}\cdot t - \int_0^t k_{\mathrm{OH+DCDO}}\cdot[\mathrm{OH}]_t\cdot\mathrm{d}t\right) \tag{11}$$

in which we have introduced the loss rate coefficient for HCHO, $L = j_{HCHO} + k_{\text{dilution}} + k_{OH+HCHO}\cdot[OH]$, made use of $W(t)/[HCHO]_0 \ll 1$ and, because the time dependencies of L and W are complex but the functions well-behaved and bounded, approximated them by their average values during the experiment, $\langle L\rangle$ and $\langle W\rangle$.

The analysis of the FTIR spectra produced accurate values for the relative change in concentrations, which were subsequently analyzed according to eq 9 (acetaldehyde experiment) or eq 11 (formaldehyde experiments) using a weighted least-squares procedure that includes uncertainties in both the dependent and independent variables.[43] The uncertainty assigned each data point includes conservative estimates of a 10% relative error in the dilution contribution and a 20% relative error in the calculated loss due to reaction with OH radicals, and a 30% relative error in the calculated HCHO source term.

The observed and modeled concentration of HCHO in the chamber is plotted in Figure 5, which also includes the loss rates of HCHO due to photolysis, dilution, reaction with OH, and the wall source of HCHO. In the example the accumulated loss due to photolysis is around 85% of the total, dilution accounts for 11% of the total loss, the OH reaction for 5%, and wall production compensates for 1% of the total loss. The

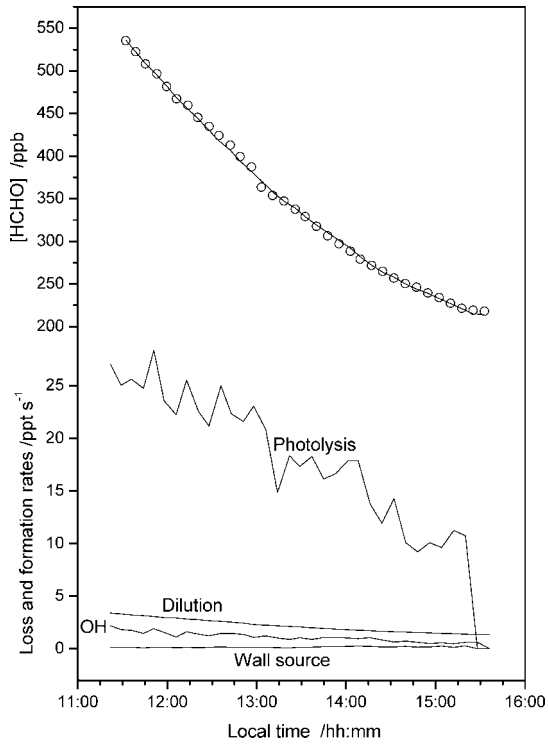

Figure 5. Observed (○) and calculated (—) concentration of HCHO in the EUPHORE chamber B on June 19, 2006 (top). Calculated loss and formation rates for HCHO (bottom). The chamber canopy was opened at 11:22 and closed at 15:36 (local time = UT+2). See text for description of the model.

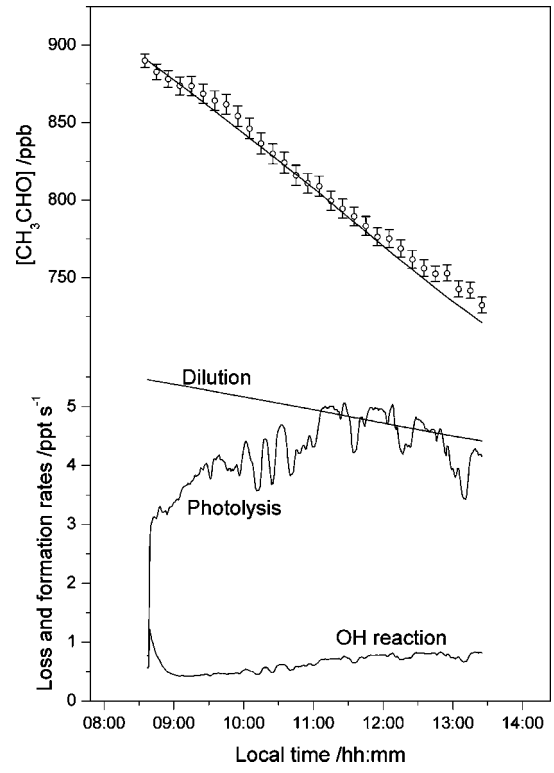

Figure 6. Observed (○) and calculated (—) concentration of CH_3CHO in the EUPHORE chamber B on June 21, 2006 (top). Calculated loss rates for CH_3CHO (bottom). The chamber canopy was opened at 08:35 and closed at 13:25 (local time = UT+2). See text for description of the model.

correction for dilution is significant, but as the dilution rate is constant (and nonfractionating) throughout each experiment, the correction does not have a large effect on the accuracy of the result. In addition to generating OH radicals during the experiment we also generate OD radicals. However, the total aldehyde loss due to reaction with OH radicals is only around 5% of the total removal in all experiments. Further, there is a large labile hydrogen reservoir, around 50−70 ppm H_2O in the gas phase (dew point −40 to −50 °C) in addition to adsorbed surface water, and isotopic scrambling will effectively minimize the OD concentration. It is therefore not important to distinguish between loss due to OH and OD in the present experiments.

Figure 6 shows the concentrations and loss rates in an acetaldehyde photolysis experiment. The photolysis rate of acetaldehyde is much smaller than that of formaldehyde, and the dilution loss rate is larger than the photolytic loss rate. The dilution rate is well determined by the SF_6 measurements and this loss term will not affect the accuracy of the result.

Figure 7 shows plots according to eq 11 of the HCHO and DCDO decays as measured by FTIR during three independent experiments. The results from the weighted least-squares analyses are summarized in Table 1. The average relative photolysis rate j_{HCHO}/j_{DCDO} is 3.15 ± 0.08, where the quoted error represents 2σ from the statistical analysis.

The corresponding plots for the three acetaldehyde experiments are shown in Figure 8. The results from weighted least-squares analyses are summarized in Table 2. The average relative photolysis rate j_{CH_3CHO}/j_{CH_3CDO} is 1.26 ± 0.03, where the quoted error represents 2σ from the statistical analysis.

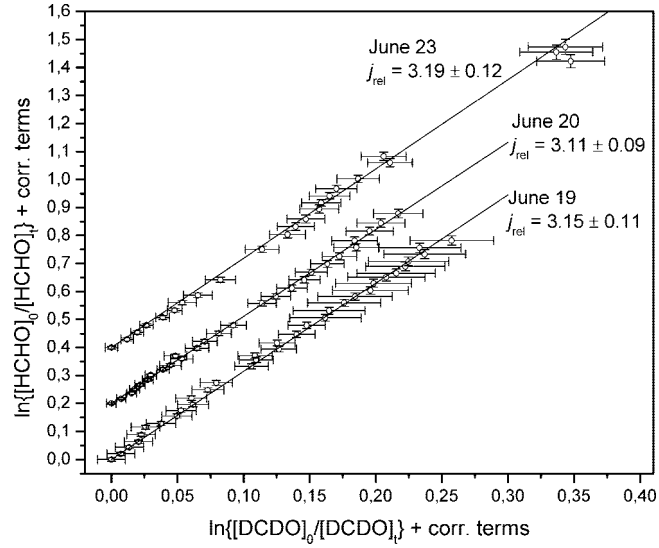

Figure 7. Decay of DCDO versus HCHO during photolysis experiments in the EUPHORE reactor as measured by FTIR. Error bars include the 1σ error from the spectral analysis and the estimated uncertainties in the correction terms given in eq 8. The average relative photolysis rate from three independent experiments is 3.15 ± 0.08 (2σ). Data offset by 0.2 and 0.4 for June 20 and 23, respectively.

4. Discussion

Since the fundamental studies of Calvert and co-workers in 1982,[44,45] the photodissociation of acetaldehyde has been extensively studied experimentally. The present study is the first determination of the isotope effect in the actinic photodissociation of acetaldehyde, j_{CH_3CHO}/j_{CH_3CDO}. In the actinic region acetaldehyde possesses a series of electronic $\pi^* \leftarrow$ n transitions, $\tilde{A}^3A'' \leftarrow \tilde{X}^1A'$ and $\tilde{A}^1A'' \leftarrow \tilde{X}^1A'$, to the triplet T_1 and singlet S_1 states. Worden reported the absolute cross sections of CH_3CHO and CH_3CDO in the 220−360 nm region and found that the integrated intensity of CH_3CDO is ca. 14% less than

TABLE 1: Summary of Relative Photolysis Rates of Formaldehyde Measured by FTIR on Three Different Days[a]

date of experiment	$[HCHO]_0/[DCDO]_0$/ppb[b]	$k_{dilution}/s^{-1}$	j_{HCHO}/j_{DCDO}
19-06-2006	600/880	6.3×10^{-6}	3.15 ± 0.11
20-06-2006	900/820	7.8×10^{-6}	3.11 ± 0.09
23-06-2006	610/600	7.0×10^{-6}	3.19 ± 0.12
weighted average			3.15 ± 0.08

[a] Errors represent 2σ derived from the statistical analyses. [b] The volume fractions of HCHO and DCDO are based on calibrated FTIR spectra from Gratien et al. [27]

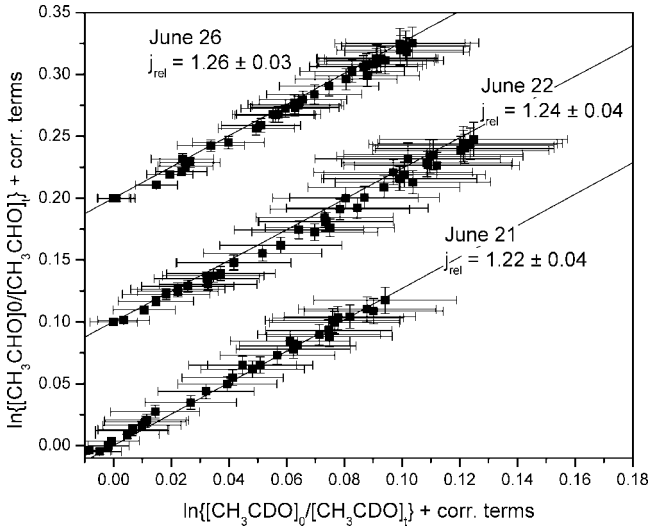

Figure 8. Decay of CH_3CDO versus CH_3CHO during photolysis experiments in the EUPHORE reactor as measured by FTIR. Error bars include the 1σ error from the spectral analysis and the estimated uncertainties in the correction terms given in eq 8. The average relative photolysis rate from three independent experiments is 1.26 ± 0.03 (2σ). Data offset by 0.1 and 0.2 for June 22 and 26, respectively.

TABLE 2: Summary of Relative Photolysis Rates of Acetaldehyde Measured by FTIR on Three Different Days[a]

Date of experiment	$[CH_3CHO]_0/[CH_3CDO]_0$/ppb	$k_{dilution}/s^{-1}$	j_{CH_3CHO}/j_{CH_3CDO}
21-06-2006	890/660	6.1×10^{-6}	1.27 ± 0.04
22-06-2006	880/670	6.6×10^{-6}	1.24 ± 0.04
26-06-2006	1100/880	6.1×10^{-6}	1.26 ± 0.03
weighted average			1.26 ± 0.03

[a] Errors represent 2σ derived from the statistical analyses.

that of CH_3CHO.[28] However, most of this difference stems from the region below 300 nm and the difference in the 290−360 nm region appears to be less than 5% (see Figure 1 in ref 28). We therefore conclude that the isotope effect in the actinic acetaldehyde photolysis is not due to the differences in the absorption spectra.

At low excitation of the S_1 state the main mechanism of decay involves internal conversion to highly vibrationally excited states of S_0;[46,47] the fluorescence lifetimes of the vibrational S_1 states in CH_3CDO are much longer than those in CH_3CHO.[47] At energies above the T_1 dissociation threshold around 316 nm the fluorescence of the vibrational S_1 states show biexponential decay as a result of intersystem crossing to the T_1 state.[48] There will obviously be differences in zero-point energies (ZPE) of CH_3CHO and CH_3CDO in the S_0 state, in the transition state to dissociation on the T_1 surface and in the radical products. Simple B3LYP/cc-pVDZ calculations of the stationary points reveal that $E_{ZPE}(TS,T_1) - E_{ZPE}(S_0)$ is around 0.5 kJ mol^{-1} larger, and $E_{ZPE}(CH_3+CHO) - E_{ZPE}(S_0)$ around 2.2 kJ mol^{-1} larger in CH_3CDO than in CH_3CHO. This alone suggests a larger CH_3CHO/CH_3CDO isotope effect in the $CH_3CHO \rightarrow CH_3 + HCO$ photodissociation on the S_0 surface than on the T_1 surface. However, in neither case can the changes in the zero point energies account for a relative photolysis rate of $j_{CH_3CHO}/j_{CH_3CDO} = 1.26$, and we conclude that the large isotope effect is related to the dynamics in the $S_1 \leftrightarrow T_1$ intersystem crossing.

The result for the formaldehyde relative photolysis rate from the present study is slightly above the previous result where the relative photolysis rate j_{HCHO}/j_{DCDO} was determined to be 3.0 ± 0.1 for experiments conducted in July 2004. However, the previous results are within the error bars of the new results. The experimental conditions for the two sets of experiments are different, and the similarity of the results demonstrates that the result is not specific to a certain set of parameters (temperature, solar zenith angle and chamber) but representative of tropospheric photolysis at 1 bar pressure. The experiment carried out with the chamber canopy closed suggests a dark source of formaldehyde of ~0.5 ppt s^{-1} in the EUPHORE chamber B, which is comparable to the additional HCHO source reported for the chamber opened to sunlight,[39] and one may speculate if the two sources are not one and the same. In any case, the magnitude of the HCHO source is insignificant in the present experiments.

The fact that the integrated UV absorption cross sections for the different formaldehyde isotopologues are equal to within the experimental uncertainty,[27] together with mechanistic information from theoretical studies,[20] implies that the differences in photolysis quantum yields are in part the result of dynamical effects,[19] just as we concluded above for acetaldehyde. From previous studies it is known that the relative photolysis rate j_{HCHO}/j_{HCDO} is about 1.58.[30] Therefore the ratio j_{HCHO}/j_{DCDO}: j_{HCHO}/j_{HCDO} is ca. 2, which means that the isotope effect is a linear function of the number of D substitutions with the broken symmetry of HCDO not having special significance. Recent work shows clearly that the isotope effects j_{HCDO}/j_{HCHO} and j_{DCDO}/j_{HCHO} decrease with decreasing pressure.[32] The mechanism involves competition between formation of molecular produces and collisional quenching, thus stratospheric photolysis of formaldehyde produces molecular hydrogen that is more highly enriched in deuterium than tropospheric photolysis. Because the fractionation factors for photolysis, radical reaction and deposition vary so much, it is expected that $\delta D(CH_2O)$ and $\delta D(CH_3CHO)$ will change greatly depending on atmospheric conditions such as the time of day and altitude (indeed $\delta D(CH_2O)$ is known to vary by hundreds of per mil,[49] providing a new technique for measuring local photochemistry.

Acknowledgment. This work is part of the ACTION project supported by the Norwegian Research Council under contracts 155959/S30 and 160270/V30. M.S.J. and E.J.K.N. thank the Copenhagen Center for Atmospheric Research supported by the Danish Natural Science Research Council and the Villum Kann Rasmussen Fund.

Supporting Information Available: Pressure (Figure S1), temperature (Figure S2), and solar flux (Figure S3) in the EUPHORE chamber B on June 19, 2006. Calculated photolysis rates j_{NO_2} (Figure S4). Concentrations of NO (Figure S5), NO_2 (Figure S6), O_3 (Figure S7), and CO (Figure S8) on the same day. This information is available free of charge via the Internet at http://pubs.acs.org.

References and Notes

(1) Anderson, L. G.; Lanning, J. A.; Barrell, R.; Miyagishima, J.; Jones, R. H.; Wolfe, P. *Atmos. Environ.* **1996**, *30*, 2113.

(2) Carlier, P.; Hannachi, H.; Mouvier, G. *Atmos. Environ.* **1986**, *20*, 2079.

(3) Singh, H.; Chen, Y.; Staudt, A.; Jacob, D.; Blake, D.; Heikes, B.; Snow, J. *Nature* **2001**, *410*, 1078.

(4) Lary, D. J.; Shallcross, D. E. *J. Geophys. Res. [Atmos.]* **2000**, *105*, 19771.

(5) Sander, S. P.; Golden, D. M.; Kurylo, M. J.; Moortgat, G. K.; Wine, P. H.; Ravishankara, A. R.; Kolb, C. E.; Molina, M. J.; Finlayson-Pitts, B. J.; Huie, R. E.; Orkin, V. L. *Chemical Kinetics and Photochemical Data for Use in Atmospheric Studies. Evaluation Number 15*; National Aeronautics and Space Administration, Jet Propulsion Laboratory: California Institute of Technology, 2006.

(6) Atkinson, R.; Baulch, D. L.; Cox, R. A.; Crowley, J. N.; Hampson, R. F.; Hynes, R. G.; Jenkin, M. E.; Rossi, M. J.; Troe, J.; Subcommittee, I. *Atmos. Chem. Phys.* **2006**, *6*, 3625.

(7) Novelli, P. C.; Lang, P. M.; Masarie, K. A.; Hurst, D. F.; Myers, R.; Elkins, J. W. *J. Geophys. Res. [Atmos.]* **1999**, *104*, 30427.

(8) Sanderson, M. G.; Collins, W. J.; Derwent, R. G.; Johnson, C. E. *J. Atmos. Chem.* **2003**, *46*, 15.

(9) Seiler, W.; Conrad, R. Contribution of tropical ecosystems to the global budgets of trace gases, especially CH4, H2, CO, and N2O. In *The Geophysiology of Amazonia*; Dickinson, R. E., Ed.; John Wiley and Sons: New York, 1987; pp 133.

(10) Warneck, P. *Chemistry of the Natural Atmosphere*, 2nd ed.; Academic Press: New York, 1999.

(11) Smith, G. D.; Molina, L. T.; Molina, M. J. *J. Phys. Chem. A* **2002**, *106*, 1233.

(12) Quay, P.; Stutsman, J.; Wilbur, D.; Snover, A.; Dlugokencky, E.; Brown, T. *Global Biogeochem. Cycles* **1999**, *13*, 445.

(13) Röckmann, T.; Jockel, P.; Gros, V.; Braunlich, M.; Possnert, G.; Brenninkmeijer, C. A. M. *Atmos. Chem. Phys.* **2002**, *2*, 147.

(14) Keppler, F.; Hamilton, J. T. G.; Brass, M.; Rockmann, T. *Nature* **2006**, *439*, 187.

(15) von Hessberg, P.; Kaiser, J.; Enghoff, M. B.; McLinden, C. A.; Sorensen, S. L.; Rockmann, T.; Johnson, M. S. *Atmos. Chem. Phys.* **2004**, *4*, 1237.

(16) Troe, J. *J. Phys. Chem. A* **2005**, *109*, 8320.

(17) Troe, J. *J. Phys. Chem. A* **2007**, *111*, 3868.

(18) Troe, J. *J. Phys. Chem. A* **2007**, *111*, 3862.

(19) Simonsen, J. B.; Rusteika, N.; Johnson, M. S.; Solling, T. I. *Phys. Chem. Chem. Phys.* **2008**, *10*, 674.

(20) Bowman, J. M.; Zhang, X. *Phys. Chem. Chem. Phys.* **2006**, *8*, 321.

(21) Feilberg, K. L.; Johnson, M. S.; Nielsen, C. J. *J. Phys. Chem. A* **2004**, *108*, 7393.

(22) D'Anna, B.; Bakken, V.; Beukes, J. A.; Nielsen, C. J.; Brudnik, K.; Jodkowski, J. T. *Phys. Chem. Chem. Phys.* **2003**, *5*, 1790.

(23) Beukes, J. A.; D'Anna, B.; Nielsen, C. J. *Asian Chem. Lett.* **2000**, *4*, 145.

(24) Beukes, J. A.; D'Anna, B.; Bakken, V.; Nielsen, C. J. *Phys. Chem. Chem. Phys.* **2000**, *2*, 4049.

(25) D'Anna, B.; Langer, S.; Ljungstrom, E.; Nielsen, C. J.; Ullerstam, M. *Phys. Chem. Chem. Phys.* **2001**, *3*, 1631.

(26) Miller, R. G. Photophysics of single vibronic levels in the Ã1A2 state of H2CO, HDCO, and D2CO. University of California, Irvine, 1975.

(27) Gratien, A.; Nilsson, E.; Doussin, J.-F.; Johnson, M. S.; Nielsen, C. J.; Picquet-Varrault, B.; Stenstrøm, Y. *J. Phys. Chem. A* **2007**, *111*, 11506.

(28) Worden, E. F. *Spectrochim. Acta* **1966**, *22*, 21.

(29) Feilberg, K. L.; D'Anna, B.; Johnson, M. S.; Nielsen, C. J. *J. Phys. Chem. A* **2005**, *109*, 8314.

(30) Feilberg, K. L.; Johnson, M. S.; Bacak, A.; Röckmann, T.; Nielsen, C. J. *J. Phys. Chem. A* **2007**, 111.

(31) Rhee, T. S.; Brenninkmeijer, C. A. M.; Röckmann, T. *Atmos. Chem. Phys.* **2008**, *8*, 1353.

(32) Nilsson, E. J. K.; Andersen, V. F.; Skov, H.; Johnson, M. S. Work in progress.

(33) Gerst, S.; Quay, P. *J. Geophys. Res. [Atmos.]* **2001**, *106*, 5021.

(34) Nilsson, E.; Johnson, M. S.; Taketani, F.; Matsumi, Y.; Hurley, M. D.; Wallington, T. J. *Atmos. Chem. Phys.* **2007**, *7*, 5873.

(35) Co, D. T.; Hanisco, T. F.; Anderson, J. G.; Keutsch, F. N. *J. Phys. Chem. A* **2005**, *109*, 10675.

(36) Pope, F. D.; Smith, C. A.; Ashfold, M. N. R.; Orr-Ewing, A. J. *Phys. Chem. Chem. Phys.* **2005**, *7*, 79.

(37) Smith, C. A.; Pope, F. D.; Cronin, B.; Parkes, C. B.; Orr-Ewing, A. J. *J. Phys. Chem. A* **2006**, *110*, 11645.

(38) Limao-Vieira, P.; Eden, S.; Mason, N. J.; Hoffmann, S. V. *Chem. Phys. Lett.* **2003**, *376*, 737.

(39) Zador, J.; Turanyi, T.; Wirtz, K.; Pilling, M. J. *J. Atmos. Chem.* **2006**, *55*, 147.

(40) Griffith, D. W. T. *Appl. Spectrosc.* **1996**, *50*, 59.

(41) Rothman, L. S.; Jacquemart, D.; Barbe, A.; Benner, D. C.; Birk, M.; Brown, L. R.; Carleer, M. R.; Chackerian, C.; Chance, K.; Coudert, L. H.; Dana, V.; Devi, V. M.; Flaud, J. M.; Gamache, R. R.; Goldman, A.; Hartmann, J. M.; Jucks, K. W.; Maki, A. G.; Mandin, J. Y.; Massie, S. T.; Orphal, J.; Perrin, A.; Rinsland, C. P.; Smith, M. A. H.; Tennyson, J.; Tolchenov, R. N.; Toth, R. A.; Vander Auwera, J.; Varanasi, P.; Wagner, G. *J. Quantum Spectrosc. Radiat. Transfer* **2005**, *96*, 139.

(42) Bloss, C.; Wagner, V.; Bonzanini, A.; Jenkin, M. E.; Wirtz, K.; Martin-Reviejo, M.; Pilling, M. J. *Atmos. Chem. Phys.* **2005**, *5*, 623.

(43) York, D. *Can. J. Phys.* **1966**, *44*, 1079.

(44) Horowitz, A.; Kershner, C. J.; Calvert, J. G. *J. Phys. Chem.* **1982**, *86*, 3094.

(45) Horowitz, A.; Calvert, J. G. *J. Phys. Chem.* **1982**, *86*, 3105.

(46) Hansen, D. A.; Edward, K. C. L. *J. Chem. Phys.* **1975**, *63*, 3272.

(47) Noble, M.; Lee, E. K. C. *J. Chem. Phys.* **1984**, *80*, 134.

(48) Leu, G.-H.; Huang, C.-L.; Lee, S.-H.; Lee, Y.-C.; Chen, I. C. *J. Chem. Phys.* **1998**, *109*, 9340.

(49) Rice, A. L.; Quay, P. D. *Anal. Chem.* **2006**, *78*, 6320.

JP811113C